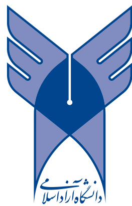
Islamic Azad University

Journal of
Optoelectronical Nanostructures

Winter 2024 / Vol. 9, No. 1

Research Paper

Defective HfS2 nanoribbons: the influence of vacancy defects and different atoms at the edge on this material with the first principle calculations

Mazdak Ghaedsharafi[1], Mohammad Reza Moslemi*[,2], Farshad Pesaran[1]

[1] Department of Electrical Engineering, Shiraz Branch, Islamic Azad University, Shiraz, Iran
[2] Department of Electrical Engineering, Zarghan Branch, Islamic Azad University, Zarghan, Iran

Received: 3 Jan. 2024
Revised: 7 Feb. 2024
Accepted: 20 Feb. 2024
Published: 15 Mar. 2024

Use your device to scan and read the article online

Keywords:
Transition Metal Dichalcogenides (TMD), HfS_2 Nanoribbon, Density Functional Theory.

Abstract:
Recently, various outstanding two-dimensional (2D) semiconductors have been studied. Some experimental and theoretical research works reveal that 2D-HfS_2 can be a good candidate to substitute with the silicon in nanoelectronics due to its acceptable band gap. First, the influence of different edge atoms i.e. H (hydrogen) and O (oxygen) on two zigzag and armchair HfS_2 nanoribbons is investigated with the first principle calculations. Second, various types of vacancy defects such as 1Hf, 2Hf, 1S, 2S-1, 2S-2, 2S-3, 3S-1, 3S-2, 6S, and 1Hf+1S are applied to the pristine zigzag and armchair nanoribbon structures to investigate their electronic and transport behaviors changes. The calculated results reveal that all edge passivated structures are stable while the edge passivated structures with hydrogen atoms are more energy favorable. Moreover, some zigzag defective structures behave as metal while the armchair ones are semiconductor. The electronic property of HfS_2 material is promising for its future applications in nanoelectronics.

Citation: Mazdak Ghaedsharafi, Mohammad Reza Moslemi, Farshad Pesaran. Defective HfS2 nanoribbons: the influence of vacancy defects and different atoms at the edge on this material with the first principle calculations. **Journal of Optoelectronical Nanostructures. 2024; 9 (1): 64- 78. DOI: 10.30495/JOPN.2024.32605.1304**

***Corresponding author:** Mohammad Reza Moslemi
Address: Department of Electrical Engineering, Zarghan Branch, Islamic Azad University, Zarghan, Iran. **Tell:** 00989173058574 **Email:** Moslemi_mr@yahoo.com

1. INTRODUCTION

Recently, two-dimensional semiconductors have been attracted significant attention and scientific researchers' focus due to their vast diversity properties and characteristics [1, 2]. One of the best candidates for optoelectronic and nanoelectronics properties are transition metal dichalcogenides semiconductors (TMDs) i. e. hafnium disulfide (HfS2), tungsten disulfide (WS2), and molybdenum disulfide (MoS2) [3-5]. So that, the MoS2 and WS2 have direct band gaps which categorized at the visible range while HfS2 monolayer represents the indirect band gap and also exciting electronic and optical properties with sandwich layered structure [6, 7]. Moreover, the octahedral symmetry HfS2 (1T) monolayer is a direct semiconductor (E_g= 1.29 eV), and it illustrates alternative significant properties i. e. chemical stability, reasonable band gap, mechanical flexibility, and ultrahigh room temperature carrier mobility [6, 8, 9], such promising properties make this TMD useful candidate for thermoelectric, photodetectors, field-effect transistors, phototransistor, and photocatalyst [6, 10].

HfX2 (X: S and Se) is a member of the two dimensional TMDs family (the IV group of chalcogenides) which their unique properties are presented in previous surveys [11-13]. Hf-based experimental studies on the bulk and monolayer HfS2 structures have been performed and the results show that this material is highly likely prone to having current density and large electron mobility to be suitable material for electronic applications [14-19]. Moreover, first-principles calculations illustrate that the increasing thickness and tensile strain result in a slight increase of bandgap [11, 20]. The band structure analysis results of HfS2 structure shows the primary effect of hafnium atoms on the conduction band and the sulfur atoms on the valence band [21]. Moreover, previous investigations reveal that the T-HfS2 structure is the most existable and energy favorable structure among all possible phases [22, 23].

In current research, the electronic properties of layered T-HfS2 nanoribbon structure (zigzag and armchair chiralities) and also the effect of different atoms at the edge and vacancy point defects on this structure are investigated by using first-principles methods. In this research, the zigzag and armchair nanoribbons of HfS2 structure are nominated as ZHfSNR and AHfSNR. The possible width of two ZHfSNR and AHfSNR structures (denotes as N) have considered N = 6 across the ribbon width which is the least feasible number according to the literature. First, we have applied Hydrogen and Oxygen atoms to the edge of these two chiralities and second, investigated the influence of various point vacancies (as defect) on these structures. Moreover, all electronic and electrical

behaviors of the relevant structures have been studied based on DFT calculations.

2. THEORY AND METHOD

In current research, the DFT based simulations are performed with Quantum espresso package [24] and the GGA (generalized gradient approximation) of the PBE exchange-correlation functional (Perdew-Burke-Ernzerhof) [25, 26]. The K-Point grids are set to$1\times21\times21$, $1\times1\times21$ and $1\times1\times22$ to calculate the electronic properties of HfS2 monolayer and also its zigzag and armchair nanoribbons, respectively. The cutoff energy and the residual force of the structures are set to 300 Ry and 0.05eV/Å, respectively. A vacuum space is set to 15 Å across the non-periodic directions to avoid image effects.
DFT is a reputable method for efficient and accurate calculation of ground state properties in very large systems [27-29]. Practical applications of DFT depend on the approximate exchange correlation energy. Despite the success of the LDA, the GGA modifies the performance of LDA. Alternatively, an empirical parameter-free GGA known as Perdew Burke Ernzerhof (PBE)-GGA can be constructed by assuming that the GGA obeys specified fundamental constraints. In general, the PBE-GGA function has many applications for executing real calculations and also as a foundation for functional derivatives [30-33].

3. RESULTS AND DISCUSSIONS

The influences of various atoms (no atoms, Hydrogen and Oxygen atoms) on electronic and electrical properties of two HfS2 nanoribbons (zigzag and armchair) are investigated and the calculated electronic results are illustrated in Fig. 1. The optimized atomic structures, bandstructure analysis and density of states (DOS) analysis of zigzag and armchair HfS2 monolayer nanoribbons with different edges (bare, hydrogen atoms and oxygen atoms) are illustrated in Fig. 1.
The calculated data reveal that HfS2 behaves as an indirect semiconductor and its energy bandgap is 0.99 eV (Fig. 1 and Table 1) which is in good confirmation with recent research [34]. According to Table 1 and edge formation energy calculations [35], 6ZHfSNR-O nanoribbon is the most stable structures among all with considerable semiconducting behavior (its bandgap is 0.43 eV). Moreover, 6AHfSNR-O nanoribbon (band gap = 0.58 eV) is the most stable one and possesses the more negative amount of the edge formation energy. Table 1 shows that all structures with different edges (both zigzag and armchair nanoribbons) are energy favorable and some of them illustrate very interesting semiconducting behavior. Moreover, DOS calculations are

performed to verify the effects of different edge passivation and point vacancy defects on electronic behavior of HfS2 nanoribbons.

TABLE 1
THE CALCULATED RESULTS OF THE HFS2, 6ZHFSNR, 6ZHFSNR-H, 6ZHFSNR-O, 6AHFSNR, 6AHFSNR-H, AND 6AHFSNR-O OPTIMIZED STRUCTURES

Structure	E_f (eV)	E_g (eV)	$E_{edge-formation}$ (eV)
HfS_2	-4.77	0.99	…
6ZHfSNR	-4.04	0	-4.96
6ZHfSNR-H	-5.03	0.95	-4.94
6ZHfSNR-O	-5.00	0.43	-6.76
6AHfSNR	-4.62	1.35	-2.86
6AHfSNR-H	-3.90	0	-2.62
6AHfSNR-O	-5.27	0.58	-3.70

In the following, the 6ZHfSNR and 6AHfSNR structures are considered as pristine ones. Then, the influence of different types of defects on these structures has been studied. The optimized atomic structures of 6ZHfSNR and 6AHfSNR with various types of defects i.e. 1Hf, 2Hf, 1S, 2S-1, 2S, 3S, 6S, and 1Hf+1S are illustrated in Fig. 2 and 3. The results reveal that four zigzag structures (6ZHfSNR-1Hf, 6ZHfSNR-2Hf, 6ZHfSNR-2S-2, and 6ZHfSNR-3S-2) behave as metal and others are semiconductors with very small gaps. Moreover, the lowest defect formation energies of 6ZHfSNR-1S and 6AHfSNR-1S structures reveal that they are the most energy favorable structures. The results of band and DOS calculations show that zigzag structures behave as metal and semiconductor but all defective armchair structures have band gaps especially 6AHfSNR-1Hf and 6AHfSNR-1Hf+1S structures and their E_g are 0.63 eV and 0.95 eV, respectively. Table 2 presents all calculated data.

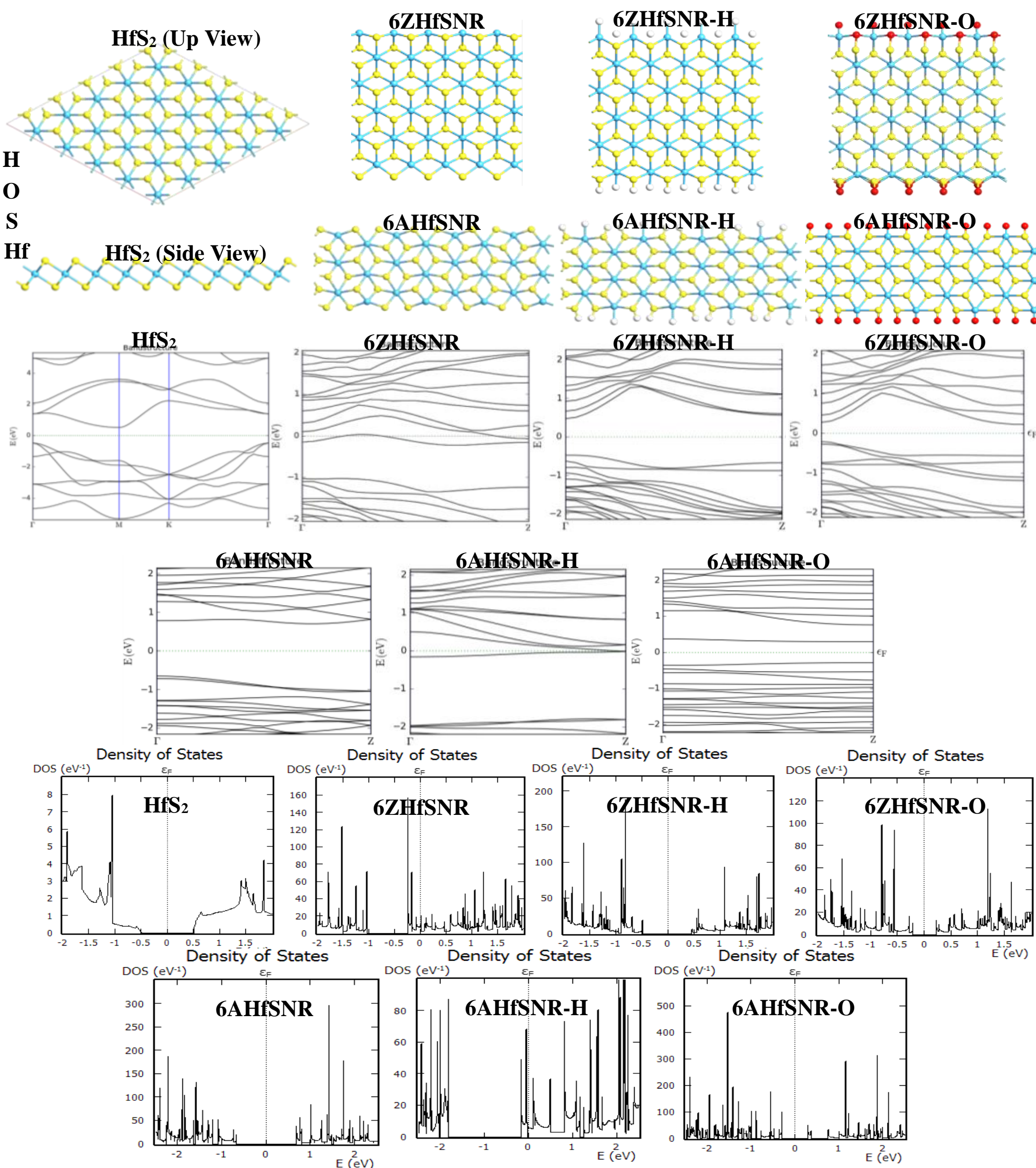

Fig. 1. The relaxed atomic structures, band and DOS results of HfS2 and their nanoribbons with different edges i. e. 6ZHfSNR, 6ZHfSNR-H, 6ZHfSNR-O, 6AHfSNR, 6AHfSNR-H, and 6AHfSNR-O structures.

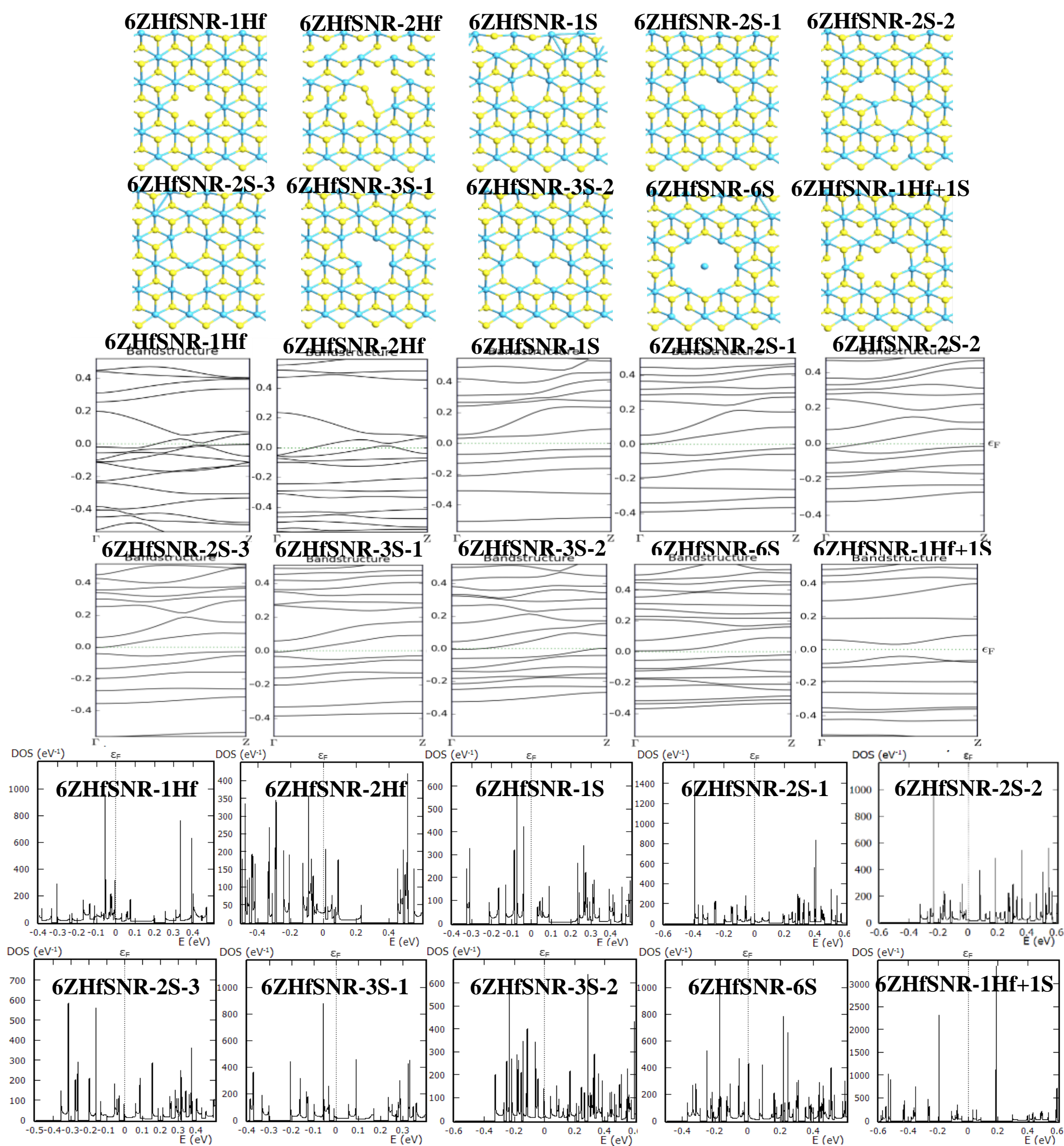

Fig. 2. The optimized atomic structures, band and DOS results of 6ZHfSNR with various defects of 1Hf, 2Hf, 1S, 2S, 3S, 6S, and 1Hf+1S.

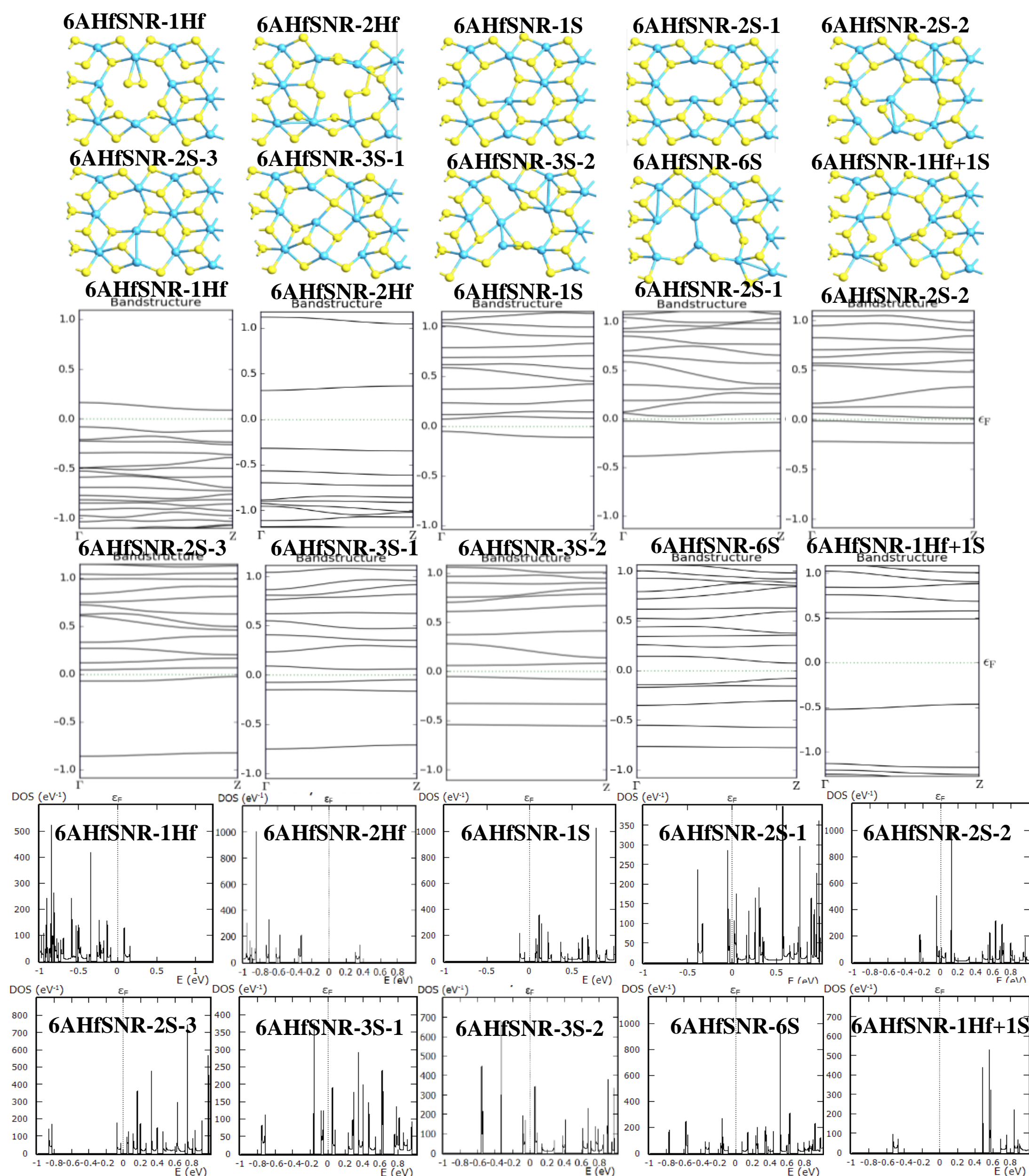

Fig. 3. The optimized atomic structures, band and DOS results of 6AHfSNR with various defects of 1Hf, 2Hf, 1S, 2S, 3S, 6S, and 1Hf+1S.

TABLE 2
THE FERMI ENERGY, BAND GAP ENERGY, AND DEFECT FORMATION ENERGY OF 6ZHFSNR AND 6AHFSNR STRUCTURES WITH VARIOUS DEFECTS OF 1HF, 2HF, 1S, 2S, 3S, 6S, AND 1HF+1S

Structure	E_f (eV)	E_g (eV)	$E_{defect-formation}$ (eV)
6ZHfSNR-1Hf	-4.48	0	5.64
6ZHfSNR-2Hf	-4.55	0	11.90
6ZHfSNR-1S	-3.84	0.07	**2.96**
6ZHfSNR-2S-1	-3.82	0.02	5.33
6ZHfSNR-2S-2	-3.78	0	5.63
6ZHfSNR-2S-3	-3.84	0.03	5.34
6ZHfSNR-3S-1	-3.79	0.02	9.73
6ZHfSNR-3S-2	-3.76	0	10.76
6ZHfSNR-6S	-3.76	0.03	23.93
6ZHfSNR-1Hf+1S	-4.39	0.07	6.93
6AHfSNR-1Hf	-5.30	0.17	8.57
6AHfSNR-2Hf	-4.96	0.63	13.75
6AHfSNR-1S	-3.87	0.11	**3.74**
6AHfSNR-2S-1	-3.85	0.07	8.50
6AHfSNR-2S-2	-3.82	0.02	7.77
6AHfSNR-2S-3	-3.85	0.09	8.13
6AHfSNR-3S-1	-3.87	0.11	10.31
6AHfSNR-3S-2	-3.90	0.11	10.59
6AHfSNR-6S	-3.73	0.15	23.42
6AHfSNR-1Hf+1S	-4.21	0.95	7.41

The presence of H and O atoms at the edge of zigzag and armchair HfS2 nanoribbons and also the defects seem to affect their electronic properties, in consequence, it is to be expected that the transport properties of such devices change significantly. In order to evaluate the electron transport characteristics (I-V) of edge passivated and defective structures, we simulated all zigzag and armchair structures by using of non-equilibrium Green’s function (NEGF) method. These relevant devices have constructed from two semi-infinite HfS2 nanoribbons, left and right leads, and a middle finite HfS2 nanoribbon (scattering region). The current-voltage curves of edge passivated structures are presented in Fig. 4 (a, b, c, d). According to the results, 6ZHfSNR and 6AHfSNR-H structures are metal and show drastic current by applying bias voltage and other structures behave as semiconductors. The calculated curves and data verify the band structure analysis. Moreover, the current-voltage characteristics of defective structures are depicted in Fig. 5 (a, b) and according to the results, the defective structures follow the electronic behavior of the

pristine structures so that zigzag structures show metallic behavior to some extent and armchair ones act as semiconductors. Plus, applying defects change the amount of current significantly. The largest values of current belong to the 6ZHfSNRand 6AHfSeNR-6S. The results are also in suitable confirmation with the electronic properties in Table 2. The negative differential resistance (NDR) shown in the calculated current of some structures is promising for further nanoelectronics and nanosensors applications.

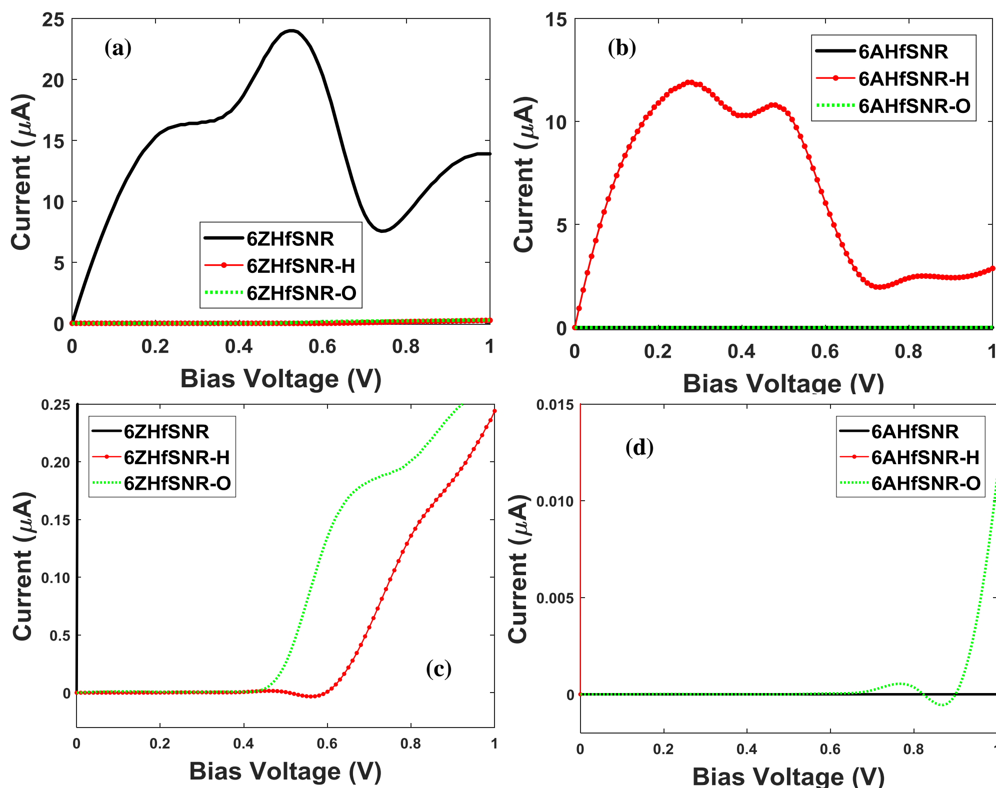

Fig. 4. The I-V characteristics of a) 6ZHfSNR, b) 6AHfSNR, c) zoom view of 6ZHfSNR and d) zoom view of 6AHfSNR structures with different atoms at the edge.

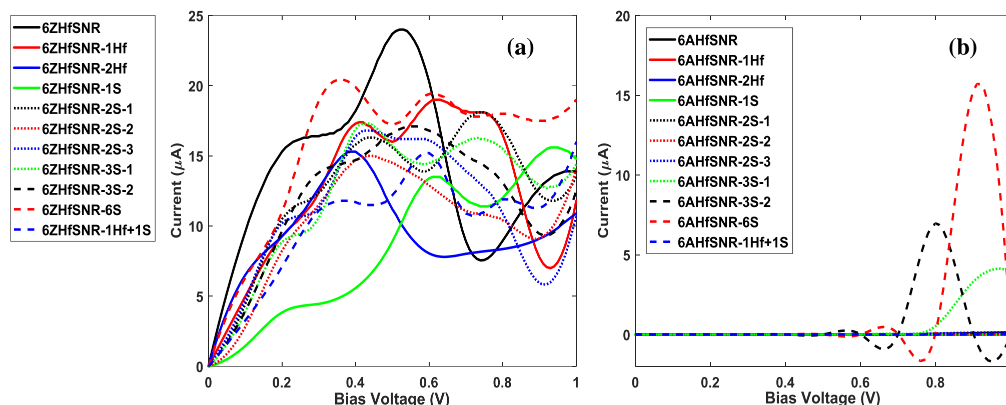

Fig. 5. The I-V characteristics of a) 6ZHfSNR and b) 6AHfSNR structures with different types of defects i.e. 1Hf, 2Hf, 1S, 2S, 3S, 6S, and 1Hf+1S.

The emergence of NDR in two-dimensional materials is the resonant tunneling phenomenon. In fact, in this phenomenon, the performance of the two-dimensional material is the same as the performance of a tunnel diode, in which the maximum amount of current occurs when the capacitance band and the conduction band move outward. Then, increasing the bias voltage causes the aforementioned bands to cross over each other and the current decreases to the minimum point (valley point), afterward the current increases normally (like a tunnel diode) [36].

4. Conclusion

The transport and electronic properties of the zigzag and armchair HfS2 nanoribbons with 6 atoms across the width in presence of H and O atoms at their edges and different types of defect are presented. The defect types are 1Hf, 2Hf, 1S, 2S (3 types), 3S (2 types), and 1Hf+1S in the pristine 6ZHfSNR and 6AHfSNR structures. According to the results, the edge passivated structures with hydrogen atoms are stable and energy favorable. Moreover, some zigzag defective structures behave as metal while the armchair ones are all semiconductor. The I-V characteristics of simulated structures verify the electronic behavior of them. Also, the observed NDR behaviour in the I-V curves is interesting and outstanding.

REFERENCES

[1] K. S. Novoselov, A. Mishchenko, A. Carvalho, and A. H. Castro Neto, *2D materials and van der Waals heterostructures*. Science 353 (6298), (2016), 9439, doi:10.1126/science.aac9439.

[2] S. Karimi Khorrami, M. Berahman, M. Sadeghi, *Carbon Monoxide Gas Sensor Based on ZrSe2 monolayer nanosheet*, Journal of Optoelectronical Nanostructures, 7(1), (2022), pp. 55-66, doi: 10.30495/jopn.2022.29652.1250.

[3] C. Yan, L. Gan, X. Zhou, J. Guo, W. Huang, J. Huang, B. Jin, J. Xiong, T. Zhai, Y. Li, *Space-confined chemical vapor deposition synthesis of ultrathin HfS2 flakes for optoelectronic application*. Adv. Funct. Mater. (2017), 27, 1702918, https://doi.org/10.1002/adfm.201702918.

[4] M. Mattinen, G. Popov, M. Vehkamaki, P. J. King, K. Mizohata, P. Jalkanen, J. Raisanen, M. Leskelä, M. Ritala, *Atomic layer deposition of emerging 2d semiconductors, HfS2 and ZrS2, for optoelectronics*. Chem. Mater. (2019), 31, 5713−5724, https://doi.org/10.1021/acs.chemmater.9b01688.

[5] K. F. Mak, J. Shan, *Photonics and optoelectronics of 2D semiconductor transition metal dichalcogenides*. Nat. Photonics (2016), 10, 216−226, doi:10.1038/nphoton.2015.282.

[6] D. Wang, X. Zhang, Z. Wang, *Recent advances in properties, synthesis and applications of two-dimensional HfS2*. J. Nanosci. Nanotechnol. (2018), 18, 7319−7334, https://doi.org/10.1166/jnn.2018.16042.

[7] U. Erkılıc, P. Solís-Fernández, H. G. Ji, K. Shinokita, Y. C. Lin, M. Maruyama, K. Suenaga, S. Okada, K. Matsuda, H. Ago, *Vapor phase selective growth of two-dimensional perovskite/WS2 heterostructures for optoelectronic applications*. ACS Appl. Mater. Interfaces, (2019), 11, 40503−40511, https://doi.org/10.1021/acsami.9b13904.

[8] J. Kang, H. Sahin, F. M. Peeters, *Mechanical properties of monolayer sulphides: a comparative study between MoS_2, HfS_2 and TiS_3*. Phys. Chem. Chem. Phys. (2015), 17, 27742−27749, https://doi.org/10.1039/C5CP04576B.

[9] Q. Zhao, Y. Guo, K. Si, Z. Ren, J. Bai, X. Xu, *Elastic, electronic, and dielectric properties of bulk and monolayer* ZrS_2*,* $ZrSe_2$*,* HfS_2*,* $HfSe_2$ *from van der Waals density-functional theory*. physica status solidi (b) (2017), 254, 1700033, http://dx.doi.org/10.1002/pssb.201700033.

[10] S. Bahrami, O. Bahrami, *Giant enhancement of second harmonic generation efficiency from monolayer group-VI transition metal dichalcogenides embedded in 1D photonic crystals*, Journal of Optoelectronical Nanostructures, 7(1), (2022), pp. 67-96, doi: 10.30495/jopn.2022.28839.1234.

[11] M. Abdulsalam, D. P. and Joubert, *Optical spectrum and excitons in bulk and monolayer* MX_2 *(M_Zr, Hf; X_S, Se)*. Phys. Status Solidi B 253 (4), (2016), 705–711. doi:10.1002/pssb.201552584.

[12] C. Cheng, J. T. Sun, X. R. Chen, S. and Meng, *Hidden spin polarization in the 1 T -phase layered transition-metal dichalcogenides* MX_2 *(M_ Zr, Hf; X _S, Se, Te)*. Sci. Bull. 63 (2), (2018), 85–91. doi:10.1016/j.scib.2017.12.003.

[13] M. Salavati, *Electronic and mechanical responses of two-dimensional* HfS_2*,* $HfSe_2$*,* ZrS_2*, and* $ZrSe_2$ *from first-principles*. Front. Struct. Civ. Eng. 13 (2), (2018), 486–494. doi:10.1007/s11709-018-0491-5.

[14] H. S. Tsai, J. W. Liou, I. Setiyawati, K. R. Chiang, C. W. Chen, C. C. Chi, et al., *Photoluminescence characteristics of multilayer* $HfSe_2$ *synthesized on sapphire using ion implantation*. Adv. Mater. Interfaces. 5 (8), (2018), 1701619. doi:10.1002/admi.201701619.

[15] M. J. Mleczko, C. F. Zhang, H. R. Lee, H. H. Kuo, B. Magyari-Kope, R. G. Moore, et al., *HfSe2 and ZrSe2: two-dimensional semiconductors with native high-κ oxides*. Sci. Adv. 3 (8), (2017), 1700481. doi:10.1126/sciadv.1700481.

[16] S. Mangelsen, P. G. Naumov, O. I. Barkalov, S. A. Medvedev, W. Schnelle, M. Bobnar, et al., *Large non saturating magneto resistance and pressure induced phase transition in the layered semimetal HfTe2*. Phys. Rev. B 96 (20), (2017), 205148. doi:10.1103/physrevb.96.205148.

[17] G. Fiori, F. Bonaccorso, G. Iannaccone, T. Palacios, D. Neumaier, A. Seabaugh, et al., *Electronics based on two-dimensional materials*. Nat. Nanotechnol. 9 (10), (2014), 768–779. doi:10.1038/nnano.2014.207.

[18] X. R. Nie, B. Q. Sun, H. Zhu, M. Zhang, D. H. Zhao, L. Chen, et al., *Impact of metal contacts on the performance of multilayer HfS2 field-effect transistors*. ACS Appl. Mater. Interfaces. 9 (32), (2017), 26996–27003. doi:10.1021/acsami.7b06160.

[19] L. Yin, K. Xu, Y. Wen, Z. Wang, Y. Huang, F. Wang, et al., *Ultrafast and ultrasensitive phototransistors based on few-layered HfSe2*. Appl. Phys. Lett. 109 (21), (2016), 213105. doi:10.1063/1.4968808.

[20] N. Wu, X. Zhao, X. Ma, Q. Xin, X. Liu, T. Wang, et al., *Strain effect on the electronic properties of 1T-HfS2 monolayer*. Phys. E Low-dimens. Syst. Nanostruct. 93, (2017), 1–5. doi:10.1016/j.physe.2017.05.008.

[21] Q. Zhao, Y. Guo, K. Si, Z. Ren, J. Bai, and X. Xu, *Elastic, electronic, and dielectric properties of bulk and monolayer ZrS_2, $ZrSe_2$, HfS_2, $HfSe_2$ from van der Waals density-functional theory*. Phys. Status Solidi (B) 254 (9), (2017), 1700033, doi:10.1002/pssb.201700033.

[22] Y. Nakata, K. Sugawara, A. Chainani, K. Yamauchi, K. Nakayama, S. Souma, et al., *Dimensionality reduction and band quantization induced by potassium intercalation in $1T-HfTe_2$*. Phys. Rev. Mater. 3 (7), (2019), 071001. doi:10.1103/physrevmaterials.3.071001.

[23] P. Yan, G. y. Gao, G. q. Ding, and D. Qin, *Bilayer MSe2 (M _ Zr, Hf) as promising two-dimensional thermoelectric materials: a first-principles study*. RSC Adv. 9 (22), (2019), 12394–12403. doi:10.1039/c9ra00586b.

[24] P. Hohenberg, and W. Kohn, *Inhomogeneous electron gas*. Phys. Rev. 136 (3B), (1964), B864–B871, DOI: 10.1103/physrev.136.b864.

[25] J. P. Perdew, and Y. Wang, *Erratum: accurate and simple analytic representation of the electron-gas correlation energy*. Phys. Rev. B 98 (7), (2018), 079904, DOI: 10.1103/physrevb.98.079904.

[26] M. Ernzerhof, and G. E. Scuseria, *Assessment of the Perdew-Burke-Ernzerhof exchange-correlation functional*. J. Chem. Phys. 110 (11), (1999), 5029–5036, DOI: 10.1063/1.478401.

[27] T. Niazkar, G. Shams, Z. soltani, *Electronic, Optical, and Thermoelectric Properties of BaFe2-xZnxAs2(x=0,1,2)orthorhombic Polymorphs: DFT Study*, Journal of Optoelectronical Nanostructures, 6(3), (2021), pp. 93-116. doi: 10.30495/jopn.2021.28945.1237.

[28] M. R. Dehghan, S. ahmadi, *Adsorption Behaviour of CO Molecule on Mg16M—O2 Nanostructures (M=Be, Mg, and Ca): A DFT Study*, Journal of Optoelectronical Nanostructures, 6(1), (2021), pp. 1-20. doi: 10.30495/jopn.2021.4538.

[29] M. Askaripour Lahiji, A. Abdolahzadeh Ziabari, *Ab–initio study of the electronic and optical traits of Na0.5Bi0.5TiO3 nanostructured thin film*, Journal of Optoelectronical Nanostructures, 4(3), (2019), pp. 47-58, https://dorl.net/dor/20.1001.1.24237361.2019.4.3.4.6.

[30] D. R Hartree, *The wave mechanics of an atom with a non-coulomb central field*, Proc. Camb. Phil. Soc 24, (1928) 89-110, doi:10.1017/S0305004100011919.

[31] P. Hohenberg, W. Kohn, *Inhomogeneous electron gas*, Phys. Rev. 136, (1964), B 864-B 871, doi:10.1103/PhysRev.136.B864.

[32] W. Kohn, L. J. Sham, *Self-consistent equations including exchange and correlation effects*, Phys. Rev. 140, (1965), A1133-A1138, doi: 10.1103/PhysRev.140.A1133.

[33] J. P. Perdew, K. Burke, M. Ernzerhof, *Generalized gradient approximation made simple*, Phys. Rev. Lett. 77, (1996), 3865-3868, doi: 10.1103/PhysRevLett.77.3865.

[34] TMD Huynh, DK Nguyen, TDH Nguyen, VK Dien, HD Pham, M-F Lin, *Geometric and Electronic Properties of Monolayer HfX2 (X _ S, Se, or Te): A First-Principles Calculation*. Front. Mater. 7:569756, (2021), doi: 10.3389/fmats.2020.569756.

[35] S. Jamalzadeh Kheirabadi, F. Behzadi, M. Sanaee, *The effect of edge passivation with different atoms on ZrSe2 nanoribbons*. Sensors and Actuators A: Physical, Volume 317, (2021), 112471, ISSN 0924-4247, https://doi.org/10.1016/j.sna.2020.112471.

[36] S. Jamalzadeh Kheirabadi, R. Ghayour, M. Sanaee, *Negative differential resistance effect in different structures of armchair graphene nanoribbon*, Diamond and Related Materials, Volume 108, (2020), 107970, ISSN 0925-9635, https://doi.org/10.1016/j.diamond.2020.107970.